


Operational definition of topological order

Amit Jamadagni^{*} and Hendrik Weimer

Institut für Theoretische Physik, Leibniz Universität Hannover, Appelstraße 2, 30167 Hannover, Germany

 (Received 7 April 2021; revised 25 August 2022; accepted 25 August 2022; published 31 August 2022)

The unrivaled robustness of topologically ordered states of matter against perturbations has immediate applications in quantum computing and quantum metrology, yet their very existence poses a challenge to our understanding of phase transitions. In particular, topological phase transitions cannot be characterized in terms of local order parameters, as it is the case with conventional symmetry-breaking phase transitions. Currently, topological order is mostly discussed in the context of nonlocal topological invariants or indirect signatures like the topological entanglement entropy. However, a comprehensive understanding of what actually constitutes topological order enabling precise quantitative statements is still lacking. Here we show that one can interpret topological order as the ability of a system to perform topological error correction. We find that this operational approach corresponding to a measurable quantity both lays the conceptual foundations for previous classifications of topological order and also leads to a successful classification in the hitherto inaccessible case of topological order in open quantum systems. We demonstrate the existence of topological order in open systems and their phase transitions to topologically trivial states. Our results demonstrate the viability of topological order in nonequilibrium quantum systems and thus substantially broaden the scope of possible technological applications.

DOI: [10.1103/PhysRevB.106.085143](https://doi.org/10.1103/PhysRevB.106.085143)

I. INTRODUCTION

Topologically ordered phases are states of matter that fall outside of Landau's spontaneous symmetry breaking paradigm and cannot be characterized in terms of local order parameters, as it is the case with conventional symmetry-breaking phase transitions. From a broad perspective, they can be classified into symmetry-protected topological order or intrinsic topological order [1]. For the former, the existence of a symmetry is required to maintain topological order, i.e., when the symmetry is broken the system immediately returns to a topologically trivial state. In some cases, topological order can be captured in terms of topological invariants such as the Chern number [2,3], but being based on single-particle wave functions, their extension to interacting systems is inherently difficult [4]. Alternatively, topological order has been discussed in terms of nonlocal order parameters often related to string order [5–8], but the main difficulty of this approach is that such string order can also be observed in topologically trivial phases [9]. From a conceptual point of view, a particularly attractive definition of topological order is the impossibility to create a certain quantum state from a product state by a quantum circuit of finite depth [10]. However, since this is equivalent to the uncomputable quantum Kolmogorov complexity [11], it has very little practical applications. Hence, most analyses of topological ordered systems have been centered around indirect signatures such as the topological entanglement entropy [12–14] or minimally entangled states [15,16], but even those quantities can prove difficult to interpret [17,18].

Here, we overcome the limitations of the previous approaches to topological order by understanding topological order as the intrinsic ability of a system to perform topological error correction, giving rise to an operational definition of topological order that can be readily computed. Our definition is thus connected to taking the robustness of topological phases as its defining property [19,20]. To make our definition mathematically precise, we call a system to be in a topologically ordered state if it can be successfully corrected by a local error correction circuit of finite depth, which gives rise to a completely generic approach to topological order, which is also closely connected to topological robustness. One key advantage of our approach is that the error correction circuit does not have to be optimal, as it only requires to reproduce the correct finite-size scaling properties, which can be expected to be universal across a topological phase transition. This puts our approach in stark contrast with the classification of topological error correction codes in terms of their threshold values [21], as the latter is a nonuniversal quantity. Symmetry protected topological order can be represented within our error correction formalism by imposing certain symmetry constraints on the error correction circuit. Compared to previous approaches to topological order, another striking advantage of our error correction method is that it corresponds to an actual observable, which can be measured in an experiment, especially in platforms where single-shot readout of the entire system is readily available [22–24].

II. OPERATIONAL DEFINITION FOR CLOSED SYSTEMS

A. From topological robustness to error correction

Let us describe how to perform a generalized construction of error correcting models for topologically ordered phases.

^{*} amit.jamadagni@itp.uni-hannover.de

We start by considering a topologically ordered phase having degenerate ground states $\{|g_\alpha\rangle\}$, where any quasilocal operator V satisfies

$$\langle g_\alpha | V | g_\beta \rangle = v \delta_{\alpha\beta} + c, \quad (1)$$

with c being either zero or vanishing in the thermodynamic limit [19]. Here, the ground-state index α defines a topological quantum number. We can take this topological quantum number to be the eigenvalue of an operator O_{topo} encoding topological order. For example, in the case of the toric code, O_{topo} is related to the nontrivial loop operators around the torus. We now separate the Hamiltonian H into a part containing the operator O_{topo} and a remaining part H_0 , by partitioning the Hilbert space into two parts, $\mathcal{H} = \mathcal{H}_0 \otimes \mathcal{H}_{\text{topo}}$, where $\mathcal{H}_{\text{topo}}$ and \mathcal{H}_0 encodes the topological and nontopological degrees of freedom, respectively. In terms of the Hamiltonian, this partitioning leads to

$$H = H_0 \otimes 1_{\text{topo}} + \lim_{h \rightarrow 0} h 1_0 \otimes O_{\text{topo}}, \quad (2)$$

where $1_{0,\text{topo}}$ refer to identities on the respective Hilbert spaces. Here, we assume that the limit $h \rightarrow 0$ is taken first and the thermodynamic limit is taken only at the end of the calculation of the error statistics. Since the topological quantum numbers describing a topological phase are good quantum numbers by construction, we have $[H, O_{\text{topo}}] = [H_0, O_{\text{topo}}] = 0$, at least in the thermodynamic limit. Importantly, H_0 has a unique ground state, as the topological ground state degeneracy of H is given by $\dim(O_{\text{topo}})$.

While it is tempting to try to analyze topological order by considering the operator O_{topo} [5], its inherent nonlocality severely limits the possibility to make general statements about its properties. For example, arguments related to spontaneous symmetry breaking do not apply and hence do not allow to treat $\langle O_{\text{topo}} \rangle$ as a topological order parameter. Therefore, we completely neglect the operator O_{topo} in the following and entirely focus our discussion on the Hamiltonian H_0 .

As already mentioned, H_0 has a unique ground state $|\psi_0\rangle$, which is also invariant under all (possibly nonlocal) symmetry transformations U_S of the original Hamiltonian H , i.e., $U_S |\psi_0\rangle |\alpha\rangle = |\psi_0\rangle |\beta\rangle$, as the topological degrees of freedom have been separated off in Eq. (2). This means that $|\psi_0\rangle$ describes a quantum paramagnet (for spin systems) or an insulator (for bosons or fermions). Without loss of generality, we will use the terminology of spins systems in the following. Crucially, a paramagnet is adiabatically connected to the ground state $|\psi_p\rangle$ of the Hamiltonian

$$H_B = B \sum_{\mu} O_{\mu}, \quad (3)$$

with quasilocal commuting operators O_{μ} and B being a constant describing an effective magnetic field. The operators O_{μ} can be chosen such that their smallest eigenvalue is zero, meaning that the ground state satisfies $O_{\mu} \equiv 0$. Here, we use the index μ to indicate that the degrees of freedom of H_B are defined on a different lattice than the original model. Note that this does not imply that H_0 can be written in the form of Eq. (3), as the fusion and braiding rules concerning *excited* states on top of $|\psi_p\rangle$ represent highly nontrivial interactions terms that are absent in Eq. (3).

In the following, we choose the state $|\psi_r\rangle = |\psi_p\rangle |\alpha\rangle$ to serve as the reference state. Which value of α is chosen to define the reference state is actually not important as it will not affect any of the O_{μ} operators. Importantly, errors with respect to the reference state are described by violations of the constraint $O_{\mu} = 0$. Since the topological phase is protected by the gap of the paramagnet, the paramagnetic phase of H_0 is equivalent to the topologically ordered phase of H .

All that is left to complete the operational definition of topological order in terms of its error correction abilities is to describe how to construct the syndrome operators O_{μ} from the reference state and how to perform the error correction. Since the error syndrome operators O_{μ} are quasilocal, it is rather straightforward to identify them once the reference state is defined. In particular one can perform an operator expansion in terms of quasilocal operators \mathcal{O}_i (defined on the original lattice) to identify the lattice sites μ and the associated operators O_{μ} in the space of excitations on top of the reference state. For example, performing an operator expansion on top of the ground state of the toric code in terms of Pauli matrices gives rise to the well-known Ising map of the anyons [25]. The set $\{O_{\mu}\}$ is the set of syndrome operators that needs to be measured before the error correction procedure can be carried out.

In the following, we assume that the syndrome operators O_{μ} have been measured M times, yielding a set of $\mathcal{O}_{\mu}^{(r)}$ measurement results, where r running from 1 to M indicates the individual measurement run. The classification of the phase then reduces to a purely classical problem: Which operations need to be applied, such that the reference state having $O_{\mu} \equiv 0$ is reached for a given configuration $\mathcal{O}_{\mu}^{(r)}$ at fixed r ? Since the configurations differ for each value of r , this introduces a statistical element to the error correction circuit. However, since the problem is classical, the required error correction circuits can be computed for very large system sizes.

Let us now refer to the circuit depth n_d as a suitable statistical measure (e.g., the mean or the variance) over all M measurement results. The required operations can be constructed from the quasilocal operators \mathcal{O}_i used to define the syndrome operators, as applying their inverse will map the system back onto the reference state. Remarkably, these operations actually describe the fusion rules of the topological phase.

Denoting by d_H the Hamming distance (or higher-dimensional equivalent) to the reference state, i.e., the number of fusion processes needed to reach the reference state, we can introduce a simple error correction strategy. From each site μ containing an error, we perform a search of the surroundings of μ to find other nearby errors. Whenever we find a configuration that allows an operation that lowers d_H , it gets carried out. Although this error correction algorithm is not necessarily optimal, it is guaranteed to result in the desired reference state as d is decreasing monotonously. Importantly, the circuit depth of the corresponding error correction circuit remains finite in the topologically ordered phase, see Appendix A, while in the trivial phase the circuit depth diverges, see Appendix B.

For the toric code discussed below, this strategy precisely yields the error correction algorithms described in

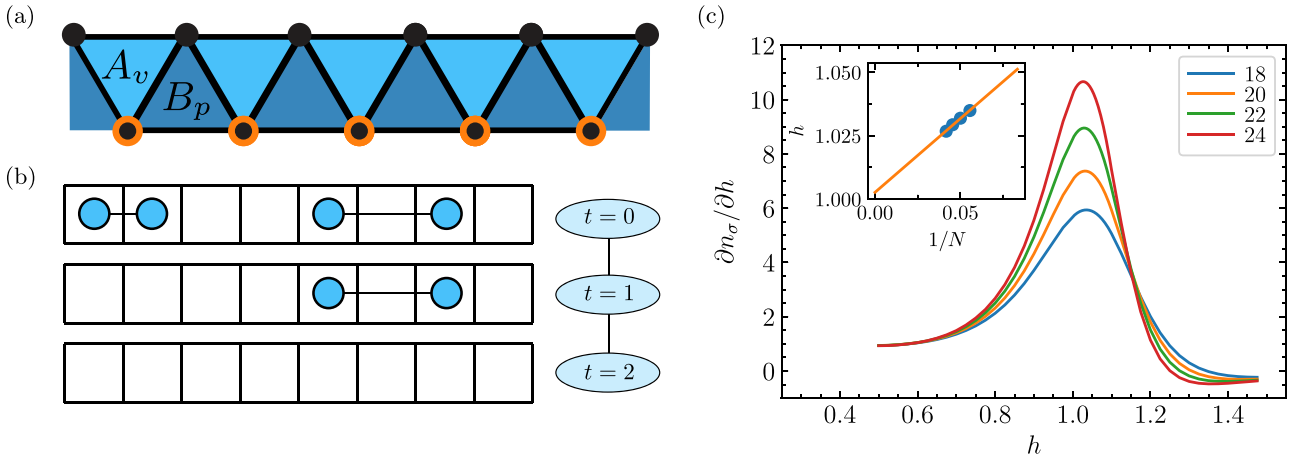


FIG. 1. Topological order in a quasi-1D toric code model. (a) The A_v and B_p operators are arranged along two rails of sites such that the perturbation on the lower rail (orange) maps onto the 1D transverse field Ising model. (b) Example of the error correction procedure for $N = 8$ Ising spins containing four errors, with the state of the system shown after t timesteps of the algorithm. The errors are fused along the horizontal strings, with the total error correction depth being $t_d = 2$. (c) Derivative $\partial n_\sigma / \partial h$ of the standard deviation n_σ of the circuit depth with respect to the perturbation strength h for different system sizes. Above the topological transition, the circuit depth diverges in the thermodynamic limit, with a finite-size scaling analysis of the position of the maximum (inset) yielding critical value of $h_c = 1.003(1)$.

Appendix D. Importantly, the same strategy can also be applied for models featuring errors described by non-Abelian anyons [26].

B. Topological order in toric code models

In our operational definition, we call a state $|\psi\rangle$ to be topologically ordered if it can be corrected to a reference state $|\psi_r\rangle$ by a local error correction circuit of finite depth. Importantly, the error correction circuit has to be capable to correct all possible errors (e.g., both phase and bit-flip errors). This differentiates topological phases from those exhibiting spontaneous symmetry breaking, as for the latter one can always find a circuit that corrects a trivial product state into a symmetry-broken state [10]. The locality of the circuit does not only refer to the actual error correction part, but also includes the circuits for syndrome measurement and classical decoding of the measurement results. For example, this implies that commonly employed error correction algorithms based on the minimum-weight perfect matching [27] cannot be employed, as they involve classical operations that are highly nonlocal. Similarly, phases related to subsystem codes characterized by nonlocal stabilizers [28] lie outside of our definition and hence are not topological, which is perfectly consistent with previous analyses [17].

The focus on the reference state $|\psi_r\rangle$ implies that our definition can be used to decide whether a given state $|\psi\rangle$ is in the same topological phase as $|\psi_r\rangle$. Hence, $|\psi\rangle$ is topologically ordered if and only if there exists a reference state $|\psi_r\rangle$ to which the state $|\psi\rangle$ can be corrected by a finite-depth circuit. We note that classifying topological phases in terms of the reference state $|\psi_r\rangle$ is actually not that different from classifying conventional Landau symmetry breaking phases in terms of local order parameters, as each order parameter also defines a set of reference states that maximize the order parameter.

To demonstrate the viability of our error correction approach in a concrete setting, we turn to the toric code model,

which serves as a paradigm for intrinsic topological order [29]. Its Hamiltonian is given by a sum over two classes of spin 1/2 operators describing four-body interactions, A_v and B_p , acting on vertices v and plaquettes p , respectively, according to

$$H_{TC} = -E_0 \left(\sum_v \underbrace{\sigma_\alpha^x \sigma_\beta^x \sigma_\gamma^x \sigma_\delta^x}_{A_v} + \sum_p \underbrace{\sigma_\mu^z \sigma_\nu^z \sigma_\rho^z \sigma_\sigma^z}_{B_p} \right), \quad (4)$$

where $\sigma_i^{x,z}$ denotes the Pauli matrix acting on site i . The robustness of topological order of the ground state can be analyzed with respect to the response of a perturbation describing a magnetic field, i.e., $H = H_{TC} - h \sum_i \sigma_i^x$. Importantly, the perturbed toric code can be mapped onto an Ising model in a transverse field using a highly nonlocal unitary transformation [30]. The phase transition from the topologically ordered to the trivial state then corresponds to the phase transition between the paramagnet and the ferromagnet in the Ising model [25]. Here, we will be interested in the case where the perturbed toric code can be mapped exactly onto the one-dimensional (1D) Ising model, which can be realized by imposing the right boundary condition [18], see Fig. 1. Our approach has the advantage that the critical point of the topological phase transitions is known to be exactly at $h_c = 1$. As there is no intrinsic topological order in 1D systems, the phase for $h < 1$ is actually a symmetry-protected topological phase, with the protected symmetry being the Z_2 symmetry of the associated Ising model. This symmetry also needs to be imposed on the error correction circuits, i.e., operations removing single anyons are forbidden. Additionally, note that the quasi-1D nature of the toric code model results in the four-body interactions in Eq. (4) being replaced by three-body interactions.

For the topological order arising in the toric code, the required topological error correction can be readily expressed in terms of the Ising variables $S_v = A_v$ and $S_p = B_p$, where

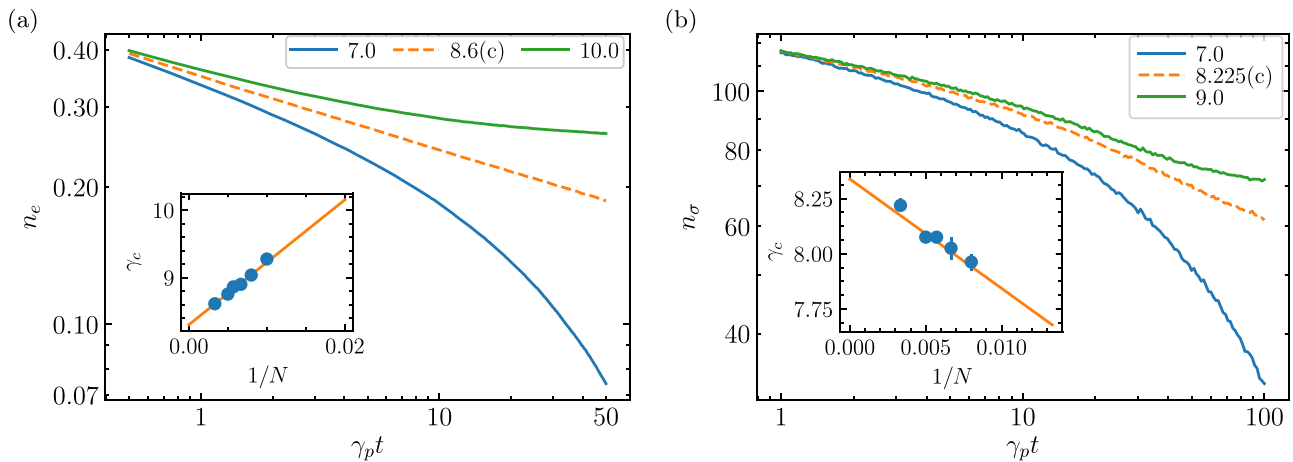


FIG. 2. Topological absorbing state transition. Error density n_e (a) and circuit depth n_σ (b) within Monte Carlo simulations for $N = 300$ sites and different values of γ , showing subcritical behavior (blue), critical behavior indicated by a vanishing curvature (orange), and supercritical behavior (green). Initial states were chosen to have maximum n_e or n_σ , respectively. Finite-size scaling leads to $\gamma_c = 8.30(2)$ [(a), inset] and $\gamma_c = 8.34(5)$ [(b), inset] in the thermodynamic limit.

each spin having $S_i^z = -1$ corresponds to the presence of an error. As a first step of the error correction algorithm, a syndrome measurement is performed, i.e., all the Ising spins are measured in their S^z basis, corresponding to the measurement of both the A_v and B_p degrees of freedom in the original toric code model. Under the perturbation, the observables S_i^z exhibit quantum fluctuations, therefore it is necessary to perform a statistical interpretation of the depth of the error correction circuit. Here, we find that the standard deviation of the circuit depth exhibits substantially better finite-size scaling behavior than the mean, hence we use the former for the detection of topological order in the following. The error correction circuit is then implemented in a massively parallel way by decorating each of the detected errors by a walker that travels through the system until it encounters another error, upon which the two errors are fused and removed from the system [31], see Appendix D for details. Figure 1 demonstrates that our error correction approach is indeed able to detect the topological phase transition, including the identification of the correct critical point at $h_c = 1$. Crucially, we want to stress that our notion of error correction is not limited to toric code models, but allows for a complete generalization both to fractional quantum Hall liquids and even to more exotic cases such as fracton order [32] in the cubic code model [33], see Appendix C 2 for details.

III. TOPOLOGICAL ORDER IN OPEN QUANTUM SYSTEMS

Let us now extend our approach to mixed quantum states, where previous works have shed some light on topological properties [34–39], but a universally applicable definition of topological order has remained elusive so far. This extension is straightforward, as the implementation of the topological error correction channel can be applied to mixed states as well. For the toric code at finite temperature [27,40,41], we can immediately see the breakdown of topological order according to our operational definition, as there is a finite probability

to create anyon pairs separated by a thermodynamically large distance, which results in a diverging circuit depth.

Next, we consider mixed states arising in open quantum systems with purely dissipative dynamics given in terms of jump operators c_i according to the Markovian quantum master equation $d\rho/dt = \sum_i c_i \rho c_i^\dagger - \{c_i^\dagger c_i, \rho\}/2$. Dissipative variants of the toric code can be constructed by considering the jump operators

$$c_i^v = \sqrt{\gamma_v} \sigma_i^z (1 - A_v)/2, \quad i \in v, \quad (5)$$

$$c_i^p = \sqrt{\gamma_p} \sigma_j^x (1 - B_p)/2, \quad j \in p, \quad (6)$$

with rates $\gamma_{v,p}$, which result in the toric code ground states being steady states of the quantum master equation [42]. As before, we now consider the robustness of topological order to an additional perturbation. Here, we will first consider again a quasi-one-dimensional model analogous to Fig. 1(a), in which the perturbation is given by

$$c_i^h = \sqrt{\gamma} \sigma_i^x (1 - B_p)/2, \quad i \in p+1, \quad (7)$$

with i being restricted to the upper rail. Note that in contrast to the jump operator of Eq. (5), this jump operator involves a spin that is part of the plaquette $p+1$ and not of the plaquette p . This multiplaquette operator leads to a heating process introducing new errors, while the jump operators of Eqs. (5) and (6) describe cooling processes that remove errors from the system. Importantly, the creation of a new error on the plaquette $p+1$ requires the existence of another error on the neighboring plaquette p . After mapping the system onto Ising variables S_i , see Appendix E for details, we obtain a purely classical master equation, despite the basis states being highly entangled. Here, we take the limit $\gamma_v \rightarrow \infty$ such that the dynamics is restricted to the Ising spins related to the B_p operators. In the basis of the Ising spins S_i , we obtain the jump operators

$$c_i^p = \sqrt{\gamma_p} S_i^x S_{i+1}^x (1 - S_i^z)/2, \quad (8)$$

$$c_i^h = \sqrt{\gamma} S_{i+1}^x (1 - S_i^z)/2. \quad (9)$$

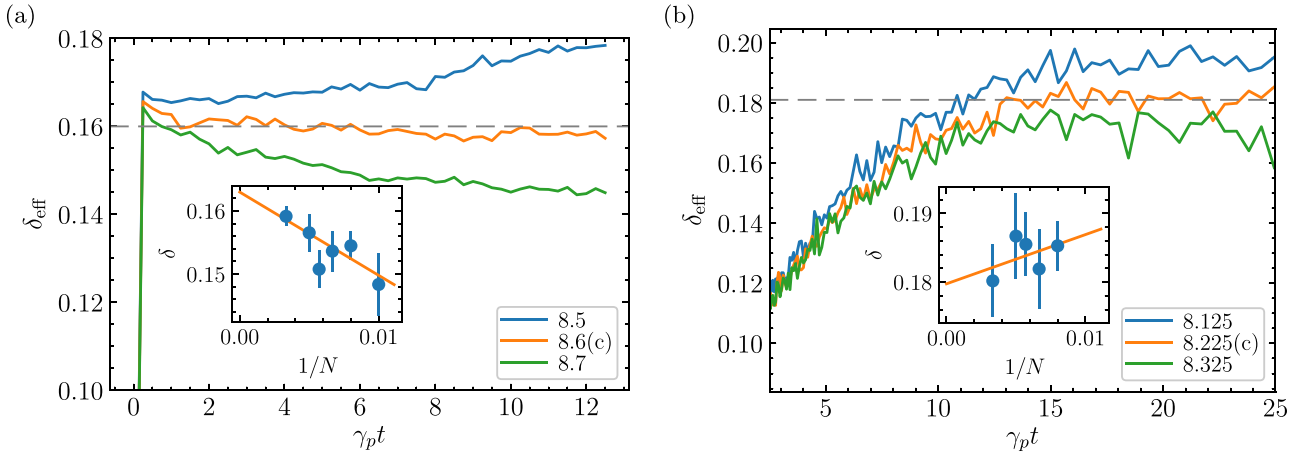


FIG. 3. Effective critical exponents according to Eq. (10) for the absorbing-active transition (a) and the topological transition (b) ($m = 4$). The critical value of the transition is taken where δ_{eff} remains constant. Error bars correspond to all values consistent with a constant value in the long time limit. Finite-size scaling leads to $\delta = 0.163(5)$ [(a), inset] and $\delta = 0.18(2)$ [(b), inset] in the thermodynamic limit. Errors are given by the sum of the uncertainty in the linear fit and the difference in δ between $m = 4$ and $m = 2$.

The resulting model falls into the well-known class of absorbing state models [43], with the toric code ground state corresponding to the absorbing state. Such absorbing state models can exhibit phase transitions to an active phase where the absorbing state is no longer reached asymptotically when starting from a different initial state. Here, we indeed find such a phase transition in the density of errors, see Fig. 2. Moreover, this absorbing-to-active transition is also accompanied by a divergence of the depth of the error correction circuit, i.e., by a topological transition to a trivial phase. We also track the critical exponent δ measuring the algebraic decay of the density of errors n_e or the circuit depth n_σ , respectively, by considering the quantity

$$\delta_{\text{eff}}(t) = -\frac{1}{\log m} \log \frac{n_{e,\sigma}(mt)}{n_{e,\sigma}(t)}, \quad (10)$$

which remains constant for a fixed value of m [43]. In the limit of large system sizes, both the critical strength for the transition and the critical exponent are in close agreement between the absorbing-to-active transition and the topological transition, see Fig. 3, belonging to the universality class of one-dimensional directed percolation ($\delta = 0.163$ [43]).

Importantly, our approach to topological order can also be readily applied to higher-dimensional systems. Here, we will be interested in a two-dimensional absorbing state model, in which both error types are present. In particular, the creation of A_v errors is conditional on the existence of a neighboring B_p error and vice versa. Hence, we consider jump operators of the form

$$c_i^{hv} = \sqrt{\gamma} \sigma_i^x (1 - A_v) / 2, \quad (11)$$

$$c_i^{hp} = \sqrt{\gamma} \sigma_i^z (1 - B_p) / 2. \quad (12)$$

Importantly, the lack of boundary processes now leads to a conservation of the parity of both types of errors. This model can be expected to be in the same universality class as two-dimensional branching-annihilating random walks with two species [44]. While the model is active for any finite γ , it exhibits nontrivial critical behavior, having an exponent $\delta = 1$

with logarithmic corrections. Figure 4 shows the data collapse for different system sizes for both the error density and the circuit depth, confirming this picture. Strikingly, the logarithmic corrections in the topological case include a quadratic term that is not present in the error density, pointing to a different critical behavior. This demonstrates that topological criticality cannot be predicted using only the properties of an accompanying conventional phase transition.

IV. SUMMARY

In summary, we have introduced an operational approach to topological order based on the ability to perform topological error correction. Our method reproduces known topological phase transitions and can be readily applied to previously inaccessible cases such as topological transitions in open quantum systems, and has the additional benefit that it corresponds to a measurable observable, which constitutes a crucial advantage over essentially unobservable entanglement measures, which are also exponentially hard to compute in the general case. Furthermore, we would like to note that our approach can be readily applied to other topologically ordered systems. For instance, we have recently demonstrated that an analogous error correction strategy can be performed within topological insulator systems [45]. Finally, our paper paves the way for many future theoretical and experimental investigations, such as the application of our approach to fracton [32,33,46] or Floquet [47,48] topological order, or the direct experimental realization of the error correction protocol presented in our paper for the development of future quantum technological devices.

ACKNOWLEDGMENTS

We thank S. Diehl and T. Osborne for fruitful discussions. This work was funded by the Volkswagen Foundation, by the Deutsche Forschungsgemeinschaft (DFG, German Research Foundation) within SFB 1227 (DQ-mat, Project No. A04),

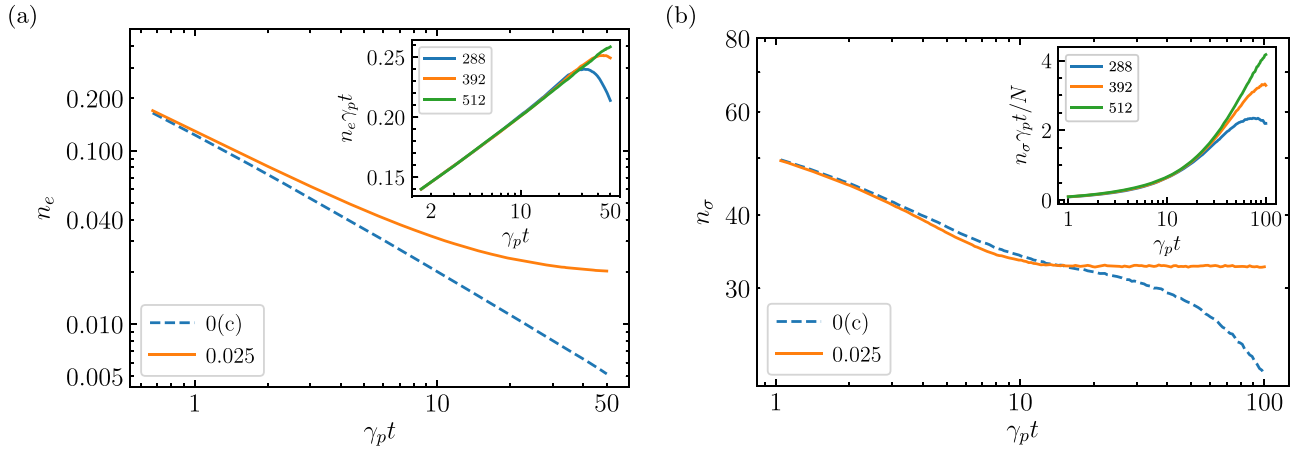


FIG. 4. Two-dimensional topological criticality. Error density n_e (a) and circuit depth n_σ (b) for $N = 512$ sites and $\gamma = 0$ (dashed) and $\gamma = 0.025 \gamma_p$ ($\gamma_p = \gamma_c$). The insets show the logarithmic corrections to a t^{-1} decay, with a linear behavior for the error density (a) and a quadratic behavior for the topological transition (b) before finite-size effects become relevant.

SPP 1929 (GiRyd), and under Germany’s Excellence Strategy – EXC-2123 QuantumFrontiers – 390837967.

APPENDIX A: MANY-BODY PERTURBATION THEORY IN THE TOPOLOGICAL PHASE

Let us now turn to a scaling analysis of the circuit depth n_d of this error correction strategy. In the topologically ordered phase, we can define all the ground states in terms of a perturbative expansion on top of the Hamiltonian H_B and its ground state $|\psi_p\rangle$, respectively [49]. Formally, the ground state of the perturbed Hamiltonian $H = H_B + \lambda V$ can be expressed as

$$|\psi\rangle = \frac{P}{\langle\psi_p|P|\psi_p\rangle} |\psi_p\rangle \quad (\text{A1})$$

using the projector $P = |\psi\rangle\langle\psi|$ given by

$$P = |\psi_p\rangle\langle\psi_p| + \sum_{k=0}^{\infty} \lambda^k A_{(k)}. \quad (\text{A2})$$

Here, the operators $A_{(n)}$ have the form

$$A_{(k)} = \sum_{(l)} -S_{l_1} V S_{l_2} V \cdots V S_{l_{k+1}}, \quad (\text{A3})$$

with the sum running over all sets of l_i satisfying $l_i \geq 0$ and $\sum_i l_i = k$. The resolvent operators S_l are given by

$$S_l = \begin{cases} |\psi_p\rangle\langle\psi_p| & \text{for } l = 0 \\ \sum_n \frac{|n\rangle\langle n|}{(E_0 - E_n)^l} & \text{for } l > 0, \end{cases} \quad (\text{A4})$$

where $|n\rangle$ are the excited states of H_B with energies E_n . Importantly, the perturbation series is convergent as long as we stay in the topological phase, as there is no closing of the energy gap. Then, we can truncate the series at k_{\max} th order, leaving an error in n_d that is exponentially small in k_{\max} , i.e., $n_d < C n_{d,k_{\max}}$, where C is a constant chosen to be independent of the system size N and $n_{d,k_{\max}}$ is the circuit depth of the state truncated at order k_{\max} [10]. Since this expression does not involve the system size, it is clear that there exists a local finite-depth error correction circuit. This finite-depth scaling

is also reached by the error correction strategy described above, as it is bounded by the largest cluster size encountered in the perturbative expansion, which again is a function of k_{\max} and not of the system size.

APPENDIX B: MAXIMALLY RANDOM ERRORS IN THE TRIVIAL PHASE

Importantly, the perturbative argument discussed above breaks down once the system is outside the topological phase, e.g., in a trivial phase, as the perturbation series diverges in this case. Note that a similar situation arises if the state is in a different topological phase than the one corresponding to the reference state. To establish the circuit depth scaling for trivial states, let us turn to the error correction properties of topological phases. We consider a topologically trivial product state of all spins pointing in the x direction. Such a state has no bit-flip errors (or higher dimensional equivalents), meaning the O_μ^{bit} describing such errors are still zero. On the other hand, the O_μ^{phase} related to phase flip errors are maximally random. This maximum randomness is reached if all configurations of the phase error syndrome $\{O_\mu^{\text{phase}}\}$ are equally likely.

In the following, we consider the mean circuit depth, i.e.,

$$\bar{n}_d = \frac{1}{M} \sum_r n_d^{(r)}, \quad (\text{B1})$$

where $n_d^{(r)}$ refers to the circuit depth for a given set of measurements $\mathcal{O}_\mu^{(r)}$. We then proceed by noting that $n_d^{(r)}$ can be bounded from below by considering a 2D torus topology containing a single error type (encoding the aforementioned phase errors) that can be removed by an m -ary fusion process, as adding more error types, higher dimensionality, or open boundaries will always increase $n_d^{(r)}$. However, treating different m separately is necessary as we will see below that there is no choice of m that leads to a minimal $n_d^{(r)}$ for all error configurations. For $m = 2$, this simplification yields the toric code model in the limit of an infinite magnetic field. Now, let us show that for the trivial state introduced above, the circuit depth diverges in the thermodynamic limit. To achieve

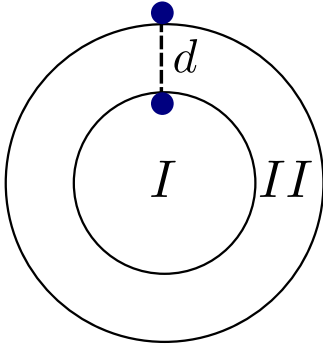


FIG. 5. Removal of the last errors. Two parts of the system I and II , each containing N/p sites are introduced. With finite probability, the last error in the part I has to be fused across an empty region II , requiring at least d steps for the error correction to complete.

this, we look at two neighboring parts within the bulk of the system, one being a circle and the other a ring surrounding the first part, see Fig. 5. Each part contains N/p sites, where p is a constant independent of the system size N . To simplify the analysis, we neglect all error correction steps that occur before we arrive at less than m errors in the two patches. Obviously, the remaining steps $n_p^{(r)}$ set again a lower bound on $n_d^{(r)}$. Since all error configurations are equally likely in the topologically trivial state under consideration, the remaining number of errors N_ε is uniformly distributed between 0 and $m - 1$. Let us now specialize on the case $N_\varepsilon = 1$, which occurs with a probability of $1/m$. Again, the one remaining error can be located in either of the two patches with a probability of $1/2$. In the case where this single error is located in the outer ring, one might get lucky and find the remaining $m - 1$ fusion partners just outside the ring and the remaining circuit depth is small. However, when the final error is located in the center patch, finding the fusion partners will require at least

$$d = (\sqrt{2} - 1) \sqrt{\frac{N}{\pi p}} \quad (\text{B2})$$

steps as the width d of the empty ring has to be crossed. Since this configuration occurs with a probability of $1/2m$, the overall circuit depth has to satisfy

$$n_d \geq \frac{\sqrt{2} - 1}{2m} \sqrt{\frac{N}{\pi p}}, \quad (\text{B3})$$

which diverges in the thermodynamic limit.

Consequently, the circuit depth n_d is always finite in the topologically ordered phase, while it diverges in the trivial phase. This demonstrates that the circuit depth can be successfully used in the classification of topologically ordered phases of matter.

APPENDIX C: ERROR CORRECTION BEYOND TORIC CODE MODELS

1. Fractional quantum Hall states

Fractional quantum Hall states are topological states of matter that occur in two-dimensional materials in large magnetic fields. They are characterized by a rational filling

fraction ν , which describes the ratio of electrons to magnetic flux quanta. Different filling fractions correspond to distinct phases of matter, and since the transition between fractional quantum Hall states does not involve any spontaneously broken symmetries, such states of matter are topologically ordered.

Identifying suitable reference states for our operational definition is straightforward, as we can employ the tremendously successful trial wave-functions introduced to describe fractional quantum Hall systems, e.g., the celebrated Laughlin states [50]. The Laughlin wave function for N particles with a filling fraction of $\nu = 1/m$ is given by

$$\psi(z_i) = \prod_{i < j} (z_i - z_j)^m e^{-\sum_{i=1}^N |z_i|^2 / 4l_B^2} \quad (\text{C1})$$

where m is an odd integer, z_i 's refers to the position of particles and $l_B = \sqrt{\frac{\hbar}{eB}}$ refers to the magnetic length. It is also possible to construct similar wave-function containing quasipoles or quasielectrons as anyonic excitations [51].

For simplicity, we consider fractional quantum Hall systems on a lattice [52–54], as it makes the connection to our operational definition easier to follow. Having specified the Laughlin state as our reference state, we need to identify the O_μ operators encoding the errors on top of the reference state and construct a suitable error correction algorithm. Crucially, quasielectrons or quasipoles can be detected due to a variation of the density in contrast to the locally uniform Laughlin state [55]. Hence, we tile the system into different regions and assign to each of these regions an index μ . The corresponding error operators are then given by

$$O_\mu = \sum_i (n_{\mu,i} - \nu), \quad (\text{C2})$$

where $n_{\mu,i}$ refers to the density at the i th site inside the region μ with the index i running over all sites contained in this region. For a successful application of the operational definition, the size of each region should be larger than the magnetic length but small compared to the system size. Note that the reference state implicitly defined by $O_\mu \equiv 0$ is not identical to the Laughlin state, but adiabatically connected to it.

Since the number of electrons is a conserved quantity, the number of quasipoles must be identical to the number of quasielectrons. We can then formulate the error correction algorithm as a procedure that fuses the quasielectrons and quasipoles in terms of their measured O_μ values according to the algorithm analogous to the one discussed in Appendix D, with a walker associated with each quasipole or quasielectron. Quasielectron and holes can be moved with the help of local potentials [54], although this step is not required to be actually implemented in order to compute the depth of the error correction circuit.

As an example, we can consider the fractional quantum Hall effect in the presence of disorder. At low disorder strengths, quasielectrons and quasipoles are bound and the error correction depth remains finite. However, when the disorder dominates, the quasielectrons and quasipoles become unbound, resulting in a diverging error correction depth signaling a trivial state. We would also like to stress that this

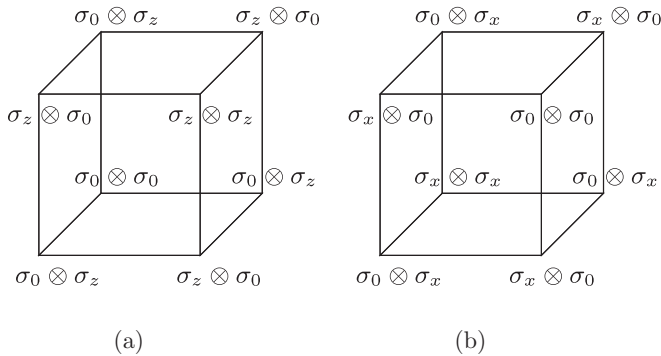


FIG. 6. Sketch of the cubic code model. Decomposition of the operators A_c (a) and B_c (b) in terms of Pauli matrices σ_x and σ_z , with σ_0 being the identity.

prescription is not limited to fractional quantum Hall states described by a Laughlin wave-function, but can be readily extended towards different classes such as Moore-Read [56] or Jain [57] states. This demonstrates that the operational definition is also capable to correctly describe topological order in fractional quantum Hall states.

2. The cubic code

The cubic code [33] is a paradigmatic model for fracton excitations, i.e., the fusion of the errors is no longer described by a linear string operator as in the toric code, but an operator that involves the sites inside the volume spanned by the errors in a fractal shape. The Hamiltonian of the cubic code has the same structure as the toric code, i.e.,

$$H = -E_0 \sum_c (A_c + B_c). \quad (\text{C3})$$

The crucial properties of the cubic code arise from the definition of the A_c and B_c operators. As shown in Fig. 6, both operators are defined in terms of the cubes c , with each vertex of the cube supporting two spin-1/2 lattice sites. Owing to the arrangement of the Pauli matrices σ_x and σ_z , flipping a single spin will result in the appearance of four errors arranged in a tetrahedron, see Fig. 7. These errors can no longer be moved around by additional flips of single spins, as such an operation would remove one error and create three additional ones, i.e., changing the number of errors and thus the energy of the system. Instead, moving errors require the application of an operator that involves the spins inside the tetrahedron in a fractal shape.

Nevertheless, error correction in the cubic code can be implemented in the same way as in Appendix D, with the reference state being one of the ground states of Eq. (C3). Here, each walker has to search for the existence of two other errors located at the vertices of a tetrahedron. If such triples of errors can be found, fusion using the fractal operator will lower the Hamming distance to the reference state, even if the fourth vertex of the tetrahedron does not contain an error.

Having specified the error correction algorithm, we can also look into the consequences for the circuit depth. In the fracton phase, the perturbative argument introduced in Sec. II A holds and the circuit depth is finite. For the trivial

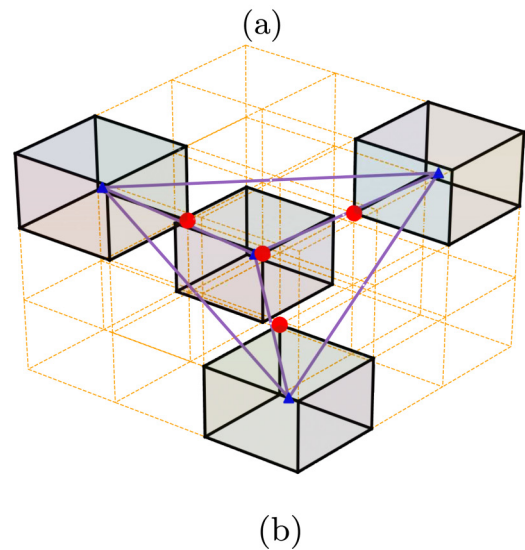
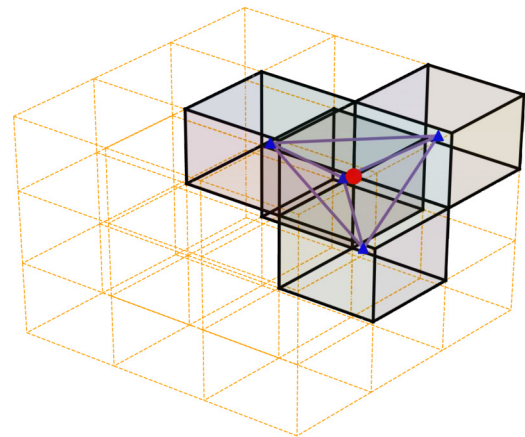


FIG. 7. Errors of the cubic code. (a) Applying a single spin-flip operator (red) to the ground state creates four errors (blue) shaped in a tetrahedron form. (b) The errors can be moved around by increasing the size of the tetrahedron by applying three additional spin-flip operators.

phase, we consider the case where all error syndromes for one error type (e.g., A_c) are equally likely. In this case, there are again configurations occurring with finite probability that require the application of a thermodynamically large fractal operator (i.e., diverging with N). From this, we conclude that we can also successfully classify fracton phases using our error correction approach.

APPENDIX D: ERROR CORRECTION CIRCUITS FOR TORIC CODE MODELS

The error correction scheme for the detection of topological order is based on the results from the error syndrome measurements, which can be cast in terms of the spin variables S_v and S_p . In cases where there are both error types being present, the error correction can be realized independently. As the figure of merit, we are interested in the depth of the classical error correction circuit, which maps the initial erroneous state onto the topologically ordered state without any errors. Our error correction procedure is massively

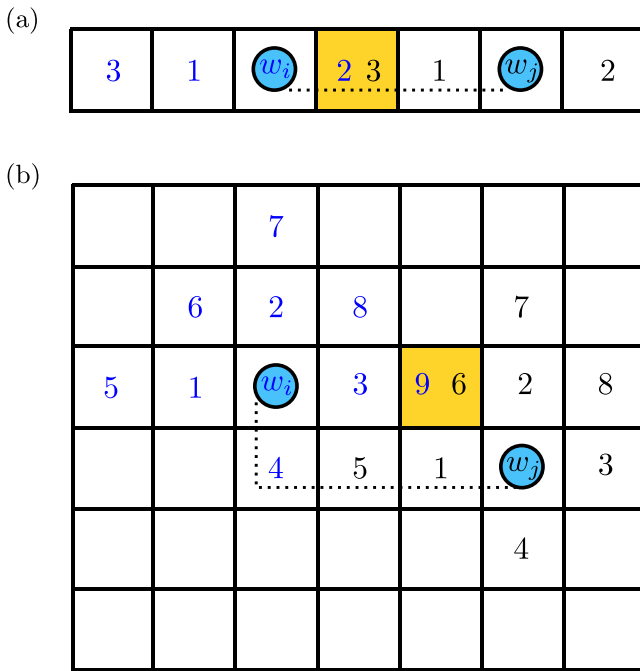


FIG. 8. Schematic representation of the error correction procedure. Two errors are associated with walkers w_i (blue) and w_j (black), located at the errors at $t = 0$. The colored numbers indicate the timestep at which a particular walker visits a site. Once a walker encounters a site already visited by the other walker (yellow), the two errors can be fused along the dotted path. In one dimension (a), the walkers alternate in a left-right pattern, in two dimensions (b), the walkers proceed in diamond-shaped patterns corresponding to a constant Manhattan distance from the initial sites.

parallelized, i.e., within a topologically ordered phase, it is able to remove a thermodynamically large number of errors in constant time. This is in stark contrast to the conventional maximum-likelihood error correction [27], as this will always require an error correction circuit whose depth scales with the system size. The same argument also holds for assessing

topological order based on circuit complexity [58], as the circuit complexity is an extensive quantity even in the topologically ordered phase.

For each error, we decorate the associated site with a walker w_i , which continuously explores the surroundings of the original site, looking for the presence of other errors. In one spatial dimension, the walker alternates between investigating sites on the left and on the right, while in two dimensions, this is generalized to continuously exploring sites with an increasing Manhattan distance to the original site, see Fig. 8. For simplicity, we assume that changing the site of a walker takes exactly one unit of time, irrespectively of the distance traveled. Once a walker encounters a site with either an error or a site previously visited by a walker w_j originating from another error, the error correction procedure starts. For this, the errors on site i and j are fused together along the shortest path, removing them and their associated walkers from the system. Here, we assume that the fusion is instantaneous, which does not modify the overall finite-size scaling properties of the error correction circuit. The error correction procedure is performed until all errors have been removed from the system. In the one-dimensional case, we also allow for errors being removed via the left or right boundary of the system, preventing the case of a single error remaining without a potential fusion partner.

APPENDIX E: ISING-MAPPED JUMP OPERATORS

After mapping the system onto Ising variables S_i , we obtain a purely classical master equation, despite the basis states being highly entangled. Here, we take the limit $\gamma_v \rightarrow \infty$ such that the dynamics is restricted to the Ising spins related to the B_p operators. In the basis of the Ising spins S_i , we obtain the jump operators

$$c_i^p = \sqrt{\gamma_p} S_i^x S_{i+1}^x (1 - S_i^z)/2,$$

$$c_i^h = \sqrt{\gamma} S_{i+1}^x (1 - S_i^z)/2.$$

-
- [1] X.-G. Wen, Colloquium: Zoo of quantum-topological phases of matter, *Rev. Mod. Phys.* **89**, 041004 (2017).
- [2] D. J. Thouless, M. Kohmoto, M. P. Nightingale, and M. den Nijs, Quantized Hall Conductance in a Two-Dimensional Periodic Potential, *Phys. Rev. Lett.* **49**, 405 (1982).
- [3] M. Kohmoto, Topological invariant and the quantization of the Hall conductance, *Ann. Phys. (NY)* **160**, 343 (1985).
- [4] L. Fidkowski and A. Kitaev, Effects of interactions on the topological classification of free fermion systems, *Phys. Rev. B* **81**, 134509 (2010).
- [5] M. den Nijs and K. Rommelse, Preroughening transitions in crystal surfaces and valence-bond phases in quantum spin chains, *Phys. Rev. B* **40**, 4709 (1989).
- [6] J. Haegeman, D. Pérez-García, I. Cirac, and N. Schuch, Order Parameter for Symmetry-Protected Phases in One Dimension, *Phys. Rev. Lett.* **109**, 050402 (2012).
- [7] F. Pollmann and A. M. Turner, Detection of symmetry-protected topological phases in one dimension, *Phys. Rev. B* **86**, 125441 (2012).
- [8] A. Elben, J. Yu, G. Zhu, M. Hafezi, F. Pollmann, P. Zoller, and B. Vermersch, Many-body topological invariants from randomized measurements in synthetic quantum matter, *Sci. Adv.* **6**, eaaz3666 (2020).
- [9] E. G. Dalla Torre, E. Berg, and E. Altman, Hidden Order in 1D Bose Insulators, *Phys. Rev. Lett.* **97**, 260401 (2006).
- [10] X. Chen, Z.-C. Gu, and X.-G. Wen, Local unitary transformation, long-range quantum entanglement, wave function renormalization, and topological order, *Phys. Rev. B* **82**, 155138 (2010).
- [11] C. E. Mora, H. J. Briegel, and B. Kraus, Quantum Kolmogorov complexity and its applications, *Int. J. Quantum Inf.* **05**, 729 (2007).

- [12] A. Kitaev and J. Preskill, Topological Entanglement Entropy, *Phys. Rev. Lett.* **96**, 110404 (2006).
- [13] M. Levin and X.-G. Wen, Detecting Topological Order in a Ground State Wave Function, *Phys. Rev. Lett.* **96**, 110405 (2006).
- [14] H.-C. Jiang, Z. Wang, and L. Balents, Identifying topological order by entanglement entropy, *Nat. Phys.* **8**, 902 (2012).
- [15] Y. Zhang, T. Grover, A. Turner, M. Oshikawa, and A. Vishwanath, Quasiparticle statistics and braiding from ground-state entanglement, *Phys. Rev. B* **85**, 235151 (2012).
- [16] W. Zhu, D. N. Sheng, and F. D. M. Haldane, Minimal entangled states and modular matrix for fractional quantum Hall effect in topological flat bands, *Phys. Rev. B* **88**, 035122 (2013).
- [17] J. C. Bridgeman, S. T. Flammia, and D. Poulin, Detecting topological order with ribbon operators, *Phys. Rev. B* **94**, 205123 (2016).
- [18] A. Jamadagni, H. Weimer, and A. Bhattacharyya, Robustness of topological order in the toric code with open boundaries, *Phys. Rev. B* **98**, 235147 (2018).
- [19] Z. Nussinov and G. Ortiz, Sufficient symmetry conditions for Topological Quantum Order, *Proc. Natl. Acad. Sci. USA* **106**, 16944 (2009).
- [20] Y. Qiu and Z. Wang, Ground subspaces of topological phases of matter as error correcting codes, *Ann. Phys.* **422**, 168318 (2020).
- [21] B. M. Terhal, Quantum error correction for quantum memories, *Rev. Mod. Phys.* **87**, 307 (2015).
- [22] S. de Léséleuc, V. Lienhard, P. Scholl, D. Barredo, S. Weber, N. Lang, H. P. Büchler, T. Lahaye, and A. Browaeys, Observation of a symmetry-protected topological phase of interacting bosons with Rydberg atoms, *Science* **365**, 775 (2019).
- [23] G. Semeghini, H. Levine, A. Keesling, S. Ebadi, T. T. Wang, D. Bluvstein, R. Verresen, H. Pichler, M. Kalinowski, R. Samajdar *et al.*, Probing topological spin liquids on a programmable quantum simulator, *Science* **374**, 1242 (2021).
- [24] K. J. Satzinger, Y.-J. Liu, A. Smith, C. Knapp, M. Newman, C. Jones, Z. Chen, C. Quintana, X. Mi, A. Dunsworth *et al.*, Realizing topologically ordered states on a quantum processor, *Science* **374**, 1237 (2021).
- [25] S. Trebst, P. Werner, M. Troyer, K. Shtengel, and C. Nayak, Breakdown of a Topological Phase: Quantum Phase Transition in a Loop Gas Model with Tension, *Phys. Rev. Lett.* **98**, 070602 (2007).
- [26] A. Schotte, G. Zhu, L. Burgelman, and F. Verstraete, Quantum Error Correction Thresholds for the Universal Fibonacci Turaev-Viro Code, *Phys. Rev. X* **12**, 021012 (2022).
- [27] E. Dennis, A. Kitaev, A. Landahl, and J. Preskill, Topological quantum memory, *J. Math. Phys.* **43**, 4452 (2002).
- [28] D. Bacon, Operator quantum error-correcting subsystems for self-correcting quantum memories, *Phys. Rev. A* **73**, 012340 (2006).
- [29] A. Y. Kitaev, Fault-tolerant quantum computation by anyons, *Ann. Phys. (NY)* **303**, 2 (2003).
- [30] L. Tagliacozzo and G. Vidal, Entanglement renormalization and gauge symmetry, *Phys. Rev. B* **83**, 115127 (2011).
- [31] J. Wootton, A simple decoder for topological codes, *Entropy* **17**, 1946 (2015).
- [32] C. Chamon, Quantum Glassiness in Strongly Correlated Clean Systems: An Example of Topological Overprotection, *Phys. Rev. Lett.* **94**, 040402 (2005).
- [33] J. Haah, Local stabilizer codes in three dimensions without string logical operators, *Phys. Rev. A* **83**, 042330 (2011).
- [34] M. B. Hastings, Topological Order at Nonzero Temperature, *Phys. Rev. Lett.* **107**, 210501 (2011).
- [35] C.-E. Bardyn, M. A. Baranov, C. V. Kraus, E. Rico, A. İmamoğlu, P. Zoller, and S. Diehl, Topology by dissipation, *New J. Phys.* **15**, 085001 (2013).
- [36] O. Viyuela, A. Rivas, and M. A. Martin-Delgado, Two-Dimensional Density-Matrix Topological Fermionic Phases: Topological Uhlmann Numbers, *Phys. Rev. Lett.* **113**, 076408 (2014).
- [37] Z. Huang and D. P. Arovas, Topological Indices for Open and Thermal Systems Via Uhlmann's Phase, *Phys. Rev. Lett.* **113**, 076407 (2014).
- [38] F. Grusdt, Topological order of mixed states in correlated quantum many-body systems, *Phys. Rev. B* **95**, 075106 (2017).
- [39] S. Roberts, B. Yoshida, A. Kubica, and S. D. Bartlett, Symmetry-protected topological order at nonzero temperature, *Phys. Rev. A* **96**, 022306 (2017).
- [40] C. Castelnovo and C. Chamon, Entanglement and topological entropy of the toric code at finite temperature, *Phys. Rev. B* **76**, 184442 (2007).
- [41] Z. Nussinov and G. Ortiz, Autocorrelations and thermal fragility of anyonic loops in topologically quantum ordered systems, *Phys. Rev. B* **77**, 064302 (2008).
- [42] H. Weimer, M. Müller, I. Lesanovsky, P. Zoller, and H. P. Büchler, A Rydberg quantum simulator, *Nat. Phys.* **6**, 382 (2010).
- [43] H. Hinrichsen, Non-equilibrium critical phenomena and phase transitions into absorbing states, *Adv. Phys.* **49**, 815 (2000).
- [44] G. Ódor, Critical branching-annihilating random walk of two species, *Phys. Rev. E* **63**, 021113 (2001).
- [45] A. Jamadagni and H. Weimer, Error-correction properties of an interacting topological insulator, [arXiv:2103.00011](https://arxiv.org/abs/2103.00011).
- [46] B. J. Brown and D. J. Williamson, Parallelized quantum error correction with fracton topological codes, *Phys. Rev. Research* **2**, 013303 (2020).
- [47] T. Kitagawa, E. Berg, M. Rudner, and E. Demler, Topological characterization of periodically driven quantum systems, *Phys. Rev. B* **82**, 235114 (2010).
- [48] N. H. Lindner, G. Refael, and V. Galitski, Floquet topological insulator in semiconductor quantum wells, *Nat. Phys.* **7**, 490 (2011).
- [49] A. Messiah, *Quantum Mechanics*, Vol. II (North-Holland, Amsterdam, 1961).
- [50] R. B. Laughlin, Anomalous Quantum Hall Effect: An Incompressible Quantum Fluid with Fractionally Charged Excitations, *Phys. Rev. Lett.* **50**, 1395 (1983).
- [51] D. Tong, Lectures on the Quantum Hall Effect, [arXiv:1606.06687](https://arxiv.org/abs/1606.06687).
- [52] F. D. M. Haldane, Model for a Quantum Hall Effect without Landau Levels: Condensed-Matter Realization of the "Parity Anomaly", *Phys. Rev. Lett.* **61**, 2015 (1988).
- [53] A. S. Sørensen, E. Demler, and M. D. Lukin, Fractional Quantum Hall States of Atoms in Optical Lattices, *Phys. Rev. Lett.* **94**, 086803 (2005).
- [54] E. Kapit and E. Mueller, Exact Parent Hamiltonian for the Quantum Hall States in a Lattice, *Phys. Rev. Lett.* **105**, 215303 (2010).

- [55] S. Manna, N. S. Srivatsa, J. Wildeboer, and A. E. B. Nielsen, Quasiparticles as detector of topological quantum phase transitions, *Phys. Rev. Research* **2**, 043443 (2020).
- [56] G. Moore and N. Read, Non-Abelions in the fractional quantum hall effect, *Nucl. Phys. B* **360**, 362 (1991).
- [57] J. K. Jain, Composite-Fermion Approach for the Fractional Quantum Hall effect, *Phys. Rev. Lett.* **63**, 199 (1989).
- [58] F. Liu, S. Whitsitt, J. B. Curtis, R. Lundgren, P. Titum, Z.-C. Yang, J. R. Garrison, and A. V. Gorshkov, Circuit complexity across a topological phase transition, *Phys. Rev. Research* **2**, 013323 (2020).